TÜBİTAK

Turkish Journal of Physics

http://journals.tubitak.gov.tr/physics/

Research Article

Turk J Phys
(2018) 42: 47 – 60

doi:10.3906/fiz-1707-8

Bessel and Bessel vortex beams generated by blunt-tip axicon

Ramazan ŞAHİN[1,2,*]
[1]Department of Physics, Faculty of Science, Akdeniz University, Antalya, Turkey
[2]National Research Institute of Electronics and Cryptology, TÜBİTAK-BİLGEM, Gebze, Turkey

Received: 14.07.2017 • **Accepted/Published Online:** 09.10.2017 • **Final Version:** 13.02.2018

Abstract: A theoretical prediction of the propagation characteristics of Laguerre–Gaussian beams after passing through a blunt-tip axicon is presented. An ideal axicon generates theoretically perfect diffraction-free and smooth-on-axis intensity Bessel beams, while experiments and calculations show that a zeroth-order Bessel beam deviates from its perfect behavior. Strong intensity modulation occurs due to interference around the center of the beam. The origin of these oscillations should be explored to increase the quality of beam shaping. This research shows that these oscillations can be reduced by stopping the beam center for a small portion or by optimizing input beam parameters. On the other hand, since they have singularity at the beam center, higher-order Bessel beams would be affected less by the bluntness of the axicon. In order to prove this idea, a series of calculations with wavelengths of 1030, 515, and 343 nm were conducted. The tip of the axicon was modeled as a hyperbola with a base angle of 0.5°. Our calculations indicate that zeroth-order Bessel beams are much more sensitive than the higher-order Bessel beams to axicon bluntness. Moreover, not only the axicon geometry and wavelength of the illuminating light, but also the input beam parameters are quite important when enhancing the quality of beam shaping.

Key words: Bessel, Bessel vortex, beam shaping, optics, laser

1. Introduction

Since they were shown as sets of diffraction-free solutions of the wave equation [1], Bessel beams have attracted much attention among researchers [2]. These beams have an electric field profile in the transverse plane given by the first kind of Bessel functions (J_n). While the zeroth-order Bessel function (J_0) has an intense central spot surrounded by concentric rings, all the others are composed of only concentric rings with the phase singularity at the beam center. Ideally, these beams consist of an infinite number of rings and so they carry infinite energy, which makes them impractical to obtain experimentally. On the other hand, very good quasi-Bessel beams were produced in prolonged distances compared to Gaussian beams of equal spot sizes [3,4].

Acquiring very small spot sizes at focus whose intensity stays high over much longer distances is useful in optical coherence tomography [5,6], atom guiding [7], or manipulating microparticles [8]. In addition, the near-field Bessel zone as well as far-field ring-shaped beam profiles can be used for drilling high aspect ratio holes [9,10]. Moreover, intense central maxima with extended focal distances could both generate plasma channels in air [11,12] and have a potential for nonlinear applications [13–15]. Bessel/Bessel vortex beams yield a submicron central spot/central ring with an extended depth of focus simultaneously, and ultrafast lasers are capable of

*Correspondence: ramazansahin@akdeniz.edu.tr

damaging any kind of materials. Therefore, direct patterning of thin films [16,17], single-layer graphene [18–20], and bulk glasses [10] at nanoscale dimensions could be achieved by joining these two techniques together.

There are some experimental techniques for generating Bessel beams. They were first obtained with a very thin annular slit [1]. Another approach is using the holographic spatial light modulator [21–23]. However, these methods are very inefficient because most of the energy of the incoming beams is stopped and cannot be transferred to the Bessel beams. Considering its simplicity and energy efficiency, using conical lenses (axicons) is the most appropriate technique in order to convert Laguerre–Gaussian beams to Bessel beams [24]. Although the majority of experimental studies consist of producing zeroth-order Bessel beams [10,16–18], recent studies show that higher-order Bessel beams [15,25,26] are of interest to the research community. Since zeroth order Bessel beams and higher-order Bessel beams possess different electric field profiles in the transverse plane, zeroth-order and higher-order beams are classified as Bessel beams and Bessel vortex beams, respectively.

In addition to the extraordinary properties of Bessel beams, recent studies report some drawbacks, such as the roundness of the axicon tip inevitably causing obvious oscillations of intensity in the propagation direction [27,28]. Since constraints during fabrication limit the precision of the axicon end, this small lens-like part of the axicon, indicated with a red curve in Figure 1, results in the refracted beam at the cone of the axicon interfering with the incoming beam [29]. However, these oscillations can be substantially reduced by stopping the small portion of the incoming beam at the center or by increasing the beam waist. These parameters not only cause or reduce intensity modulation; the wavelength of the laser may also affect the resulting Bessel beams. The calculations were extended to Bessel vortex beams and revealed that Bessel vortex beams are less prone to intensity modulations due to axicon bluntness.

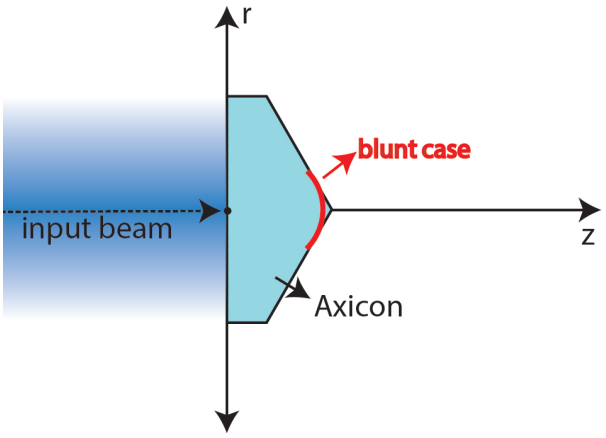

Figure 1. Axicon geometries for an ideal (ideally sharp) and blunt case (red curve). The input Gaussian beam propagates in the z-direction.

2. Results and discussion

In our analysis, we focus on the generation of Bessel and Bessel vortex beams by axicons. Ideal Bessel beams are obtained as a result of interference of a conical wavefront made by a sharp axicon. Therefore, the electrical field profile behind the axicon can be calculated by solving the Fresnel–Kirchhoff integral numerically using MATLAB. In this calculation, the electrical field profile of the incoming beam is considered to be Gaussian (TEM_{00}) for Bessel (J_0) and a first-order Laguerre–Gaussian mode (TEM_{01}) for Bessel vortex (J_1) beams. A general expression for the Laguerre–Gaussian mode is given by the following expression:

$$E_l\left(r,\Phi,0\right) \propto \left(\frac{2r^2}{w_0^2}\right)^{\frac{l}{2}} L_p^l\left(\frac{2r^2}{w_0^2}\right) e^{\left(-\frac{r^2}{w_0^2}\right)} e^{il\Phi}, \tag{1}$$

where w_0 is the beam waist and l and p are the two parameters deciding the mode. The variable l describes the charge of phase singularity, and p is proportional to the number of concentric rings in the illuminating beam. Since we focus on the generation of zeroth-order Bessel and first-order Bessel vortex beams, $l = 0$ and $p = 0$ for TEM_{00} and $l = 1$ and $p = 0$ for TEM_{01} modes. Therefore, a general expression for the Laguerre–Gaussian beam can be composed for these two modes and yields the following expressions for illuminating beams:

$$E_{00}\left(r\right) \propto e^{\left(-r^2\,/\,w_0^2\right)} \tag{2}$$

$$E_{01}\left(r\right) \propto r\, e^{\left(-r^2\,/\,w_0^2\right)} e^{i\Phi} \tag{3}$$

In Eqs. (2) and (3), E_{00} or E_{01} is the electrical field profile of the illuminating beam in the transverse plane. Since the system has cylindrical symmetry before the axicon, which makes the system independent from azimuthal angle Φ, the electric field profile behind the axicon can be obtained by evaluating the Fresnel–Kirchhoff integral, as follows:

$$E_n\left(r,z\right) \propto \frac{e^{ik\left(z\,+\,r^2\,/\,2z\right)}}{z} \int_o^\infty e^{\left(-ik\frac{r_0^2}{2z}\right)} J_n\left(krr_0/z\right)\, E\left(r_0\right) r_0\, dr_0 \tag{4}$$

Here $E_n(r,\, z)$ is the electrical field at a point $(r,\, z)$ propagating in a z-direction perpendicular to the transverse plane, $E(r_0)$ is the input electrical field including the phase retardation due to the axicon [28], λ is the wavelength of the illuminating light, and J_n is the $n\text{th}-$order Bessel function of the first kind where k is the wavenumber. To compare electrical field profiles of tailored beams from ideal (perfectly sharp) and round-tip axicons, the axicon tip was modeled as a hyperbole, as indicated in [28,30], for the blunt axicon case. Experimentally measured values were used for axicon geometry [28]. Since the only difference between an ideally sharp and a blunt-tip axicon is the tip, Bessel and Bessel vortex beams were not expected to show similar behavior after the axicon. Therefore, the analysis is divided into two parts: (i) Bessel beams and (ii) Bessel vortex beams.

2.1. Bessel beams

Ideal axicons can provide a good approximation to the zeroth order and the first kind of Bessel beams when they are illuminated with monochromatic and coherent light sources whose electrical field profiles are described by the Gaussian mathematical function in the transverse plane. In order to understand the characteristic behavior of Bessel beams, the transverse electrical field profile around the focal region of an ideal axicon was obtained, as well as its intensity in the propagation direction. Figure 2 shows the beam profiles obtained by evaluating the Fresnel–Kirchhoff integral for an ideal axicon illuminated by TEM_{00} mode.

As explained above, the intensity profile in the transverse plane includes a central maximum surrounded by concentric rings. The diameter of the central maximum does not change by propagation; its intensity stays high over much longer distances compared to the same spot sizes of Gaussian beams. Then the same calculation was repeated for the round tip axicon in which the geometry is defined as above. The intensity of central maximum oscillates a great deal in the propagation direction. Figure 3a shows the longitudinal beam profile of ideal and round-tip axicons for $\lambda = 1030$ nm and $\alpha = 0.5^\circ$ base angle. In this calculation, the

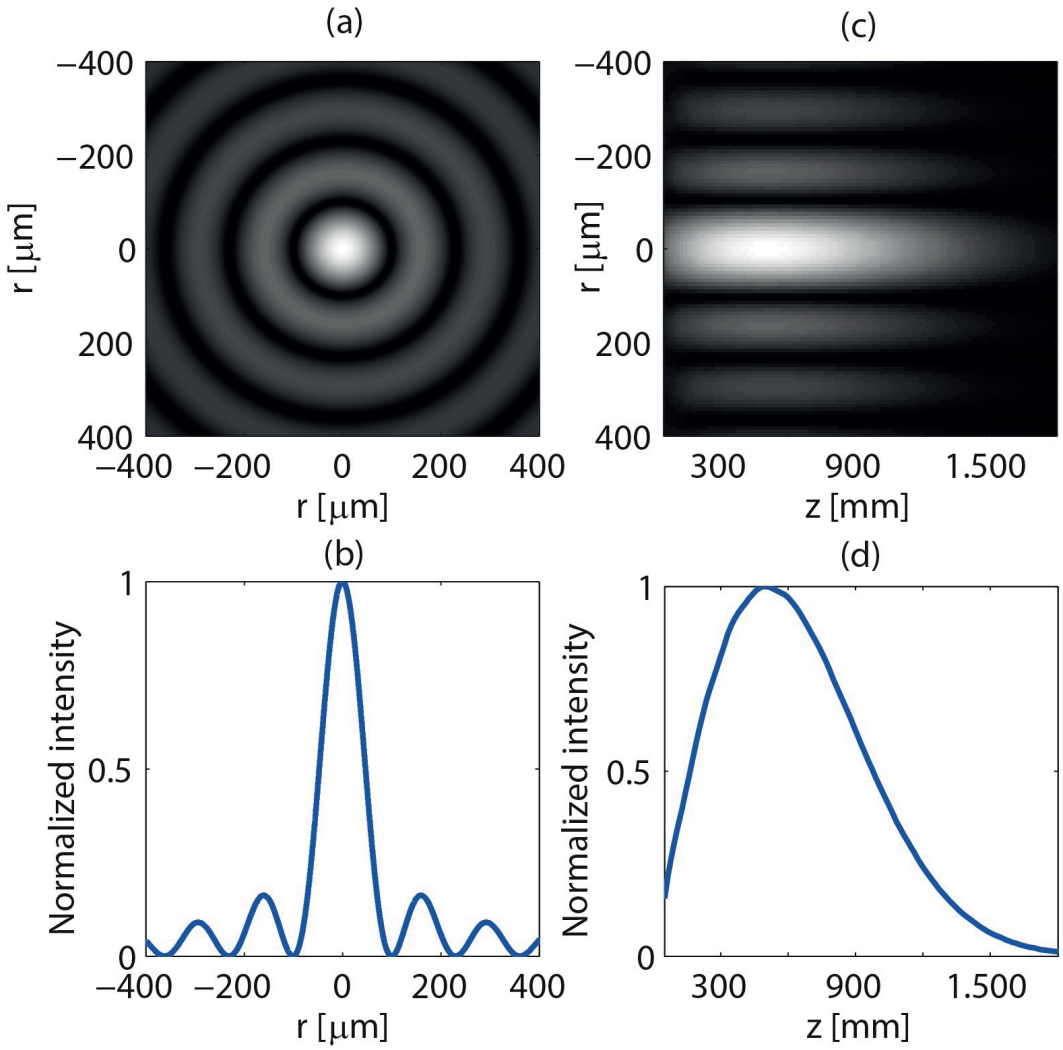

Figure 2. a) Calculated Bessel beam profile for $\lambda = 1030$ nm, $w_0 = 4$ mm, and $\alpha = 0.5^\circ$ and b) cross-section from its center. c) Intensity distribution in both transverse and longitudinal directions. d) Normalized intensity at $r = 0$ in the propagation direction for an ideal axicon.

beam waist of the input Gaussian beam is taken as $w_0 = 5$ mm. In order to see the effect of the diameter of the input beam, the same integral was evaluated for different w_0 values and the results are depicted in Figure 3b. According to our calculations, no matter what the beam waist is, the oscillations of the intensity in the propagation direction are preserved. In addition, there is a strict peak at the same position (z = 290 mm) for different w_0 values. In order to understand the source of this common peak, the beam waist was reduced to 0.5 mm. Since the tip of the axicon is round and modeled as hyperbola with a 0.86 mm radius, the axicon behaves as a typical lens for a small beam waist. Based on the lens maker's formula, the focal length of this small part was calculated as 290 mm. Another defining input parameter is the wavelength of the light. Therefore, the Fresnel–Kirchhoff integral was evaluated, taking into account axicon roundness for different wavelengths, as shown in Figure 3c. There are always high-intensity peaks at around 290 mm for three different wavelengths, which is very convenient regarding focal distance of the round lens-like part of the axicon.

The propagation properties of Bessel beams generated by ideal and round-tip axicon both in transverse

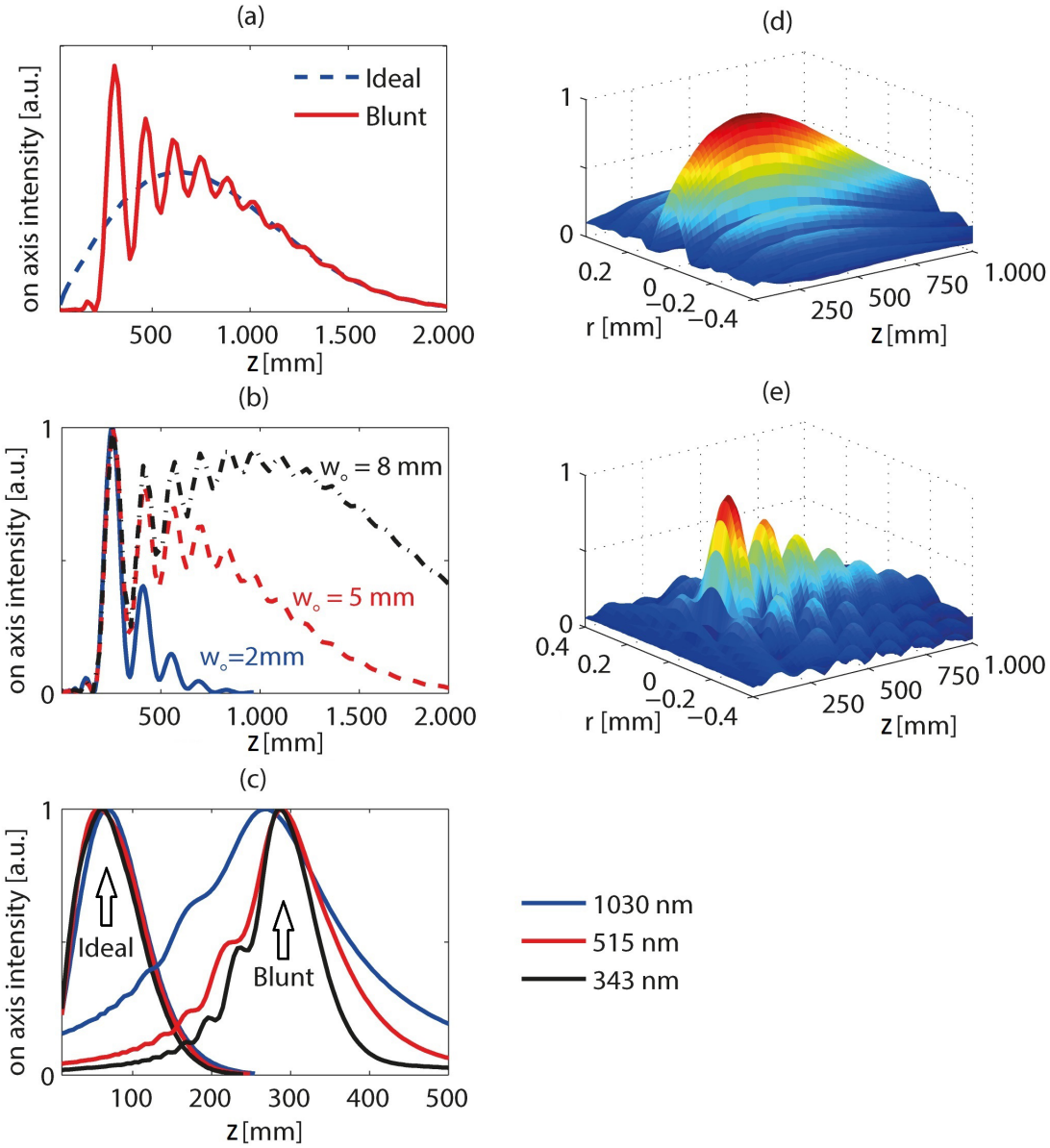

Figure 3. Intensities in the propagation direction a) for ideal and blunt-tip axicons, where $\lambda = 1030$ nm and $w_0 = 5$ mm, b) for blunt-tip axicon where $\lambda = 1030$ nm and different input beam sizes, c) for ideal and blunt-tip axicon cases where $w_0 = 0.5$ mm. d) and e) are the intensity distributions for an ideal and a blunt-tip axicon where $w_0 = 3$ mm, respectively.

and in longitudinal positions were analyzed. As seen in Figure 3d, axicon tip roundness causes strong oscillations in the propagation direction, which reduces the quality of beam shaping. Then the calculations were extended to shorter wavelengths by evaluating the same integral. For small wavelengths, the intensity oscillations are more frequent, as shown in Figure 4a. The intensity profile after axicon was calculated for different input beam radii. Figure 4b shows the obtained beam profiles. When the input beam radius is increased, intensity oscillations are consequently reduced, as the portion of the beam affected by the roundness of the axicon gets smaller. Therefore, even if a round-tip axicon is used for beam shaping, reducing intensity oscillations is possible. This has strong potential for long-depth-of-focus applications, such as generating plasma channels, fabricating waveguides with

ultrafast lasers, and manipulating nanoparticles. Since axicon bluntness is responsible for intensity oscillations, stopping the incoming beam center with a small portion at the center can be another alternative to get rid of intensity oscillations.

For comparison, beam profiles after ideal and blunt axicons without/with beam stop at the center were evaluated. Figures 5a and 5b show the intensity profiles of Bessel beams without/with a beam stop at the center of the input, whereas Figure 5c shows the intensity cross-section in the propagation direction. Although the radius of the beam stop is 0.5 mm, the oscillations in the propagation direction are much reduced, paving the way for a small amount of energy to be lost. Due to the roundness of the axicon tip, intensity at the beam center in the propagation direction is very prone to oscillations. On the other hand, one can control and reduce this drawback, provided that optimizing input beam parameters or energy transfer is compromised a little during beam shaping.

2.2. Bessel-vortex beams

In the second part of the analysis, Bessel vortex beams are employed and their propagation through ideal and blunt-tip axicons is analyzed. Different from Bessel beams, Bessel-vortex beams have a singularity at the

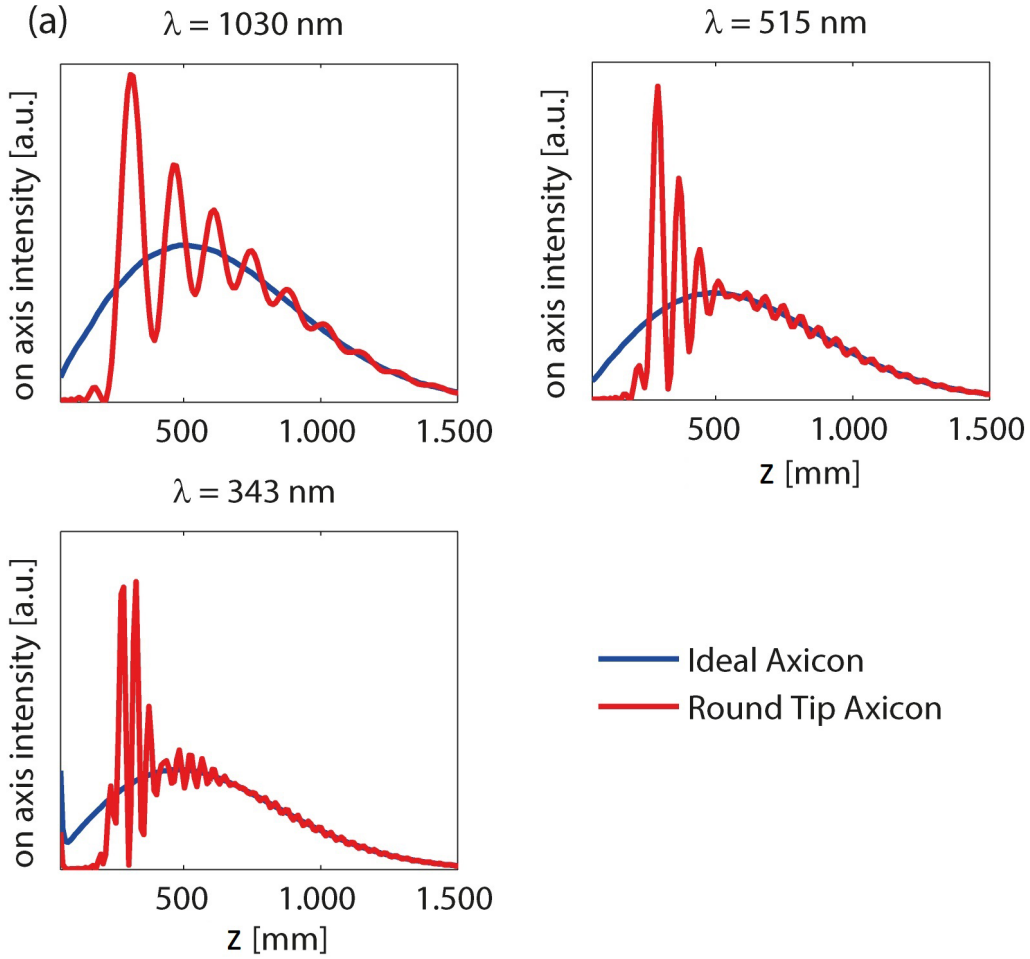

Figure 4. a) Comparison of intensities in the propagation direction for $w_0 = 4$ mm and variety of wavelengths. b) Intensity distributions for $w_0 = 2$ mm (left column) and $w_0 = 8$ mm (right column) with different wavelengths and round-tip axicon.

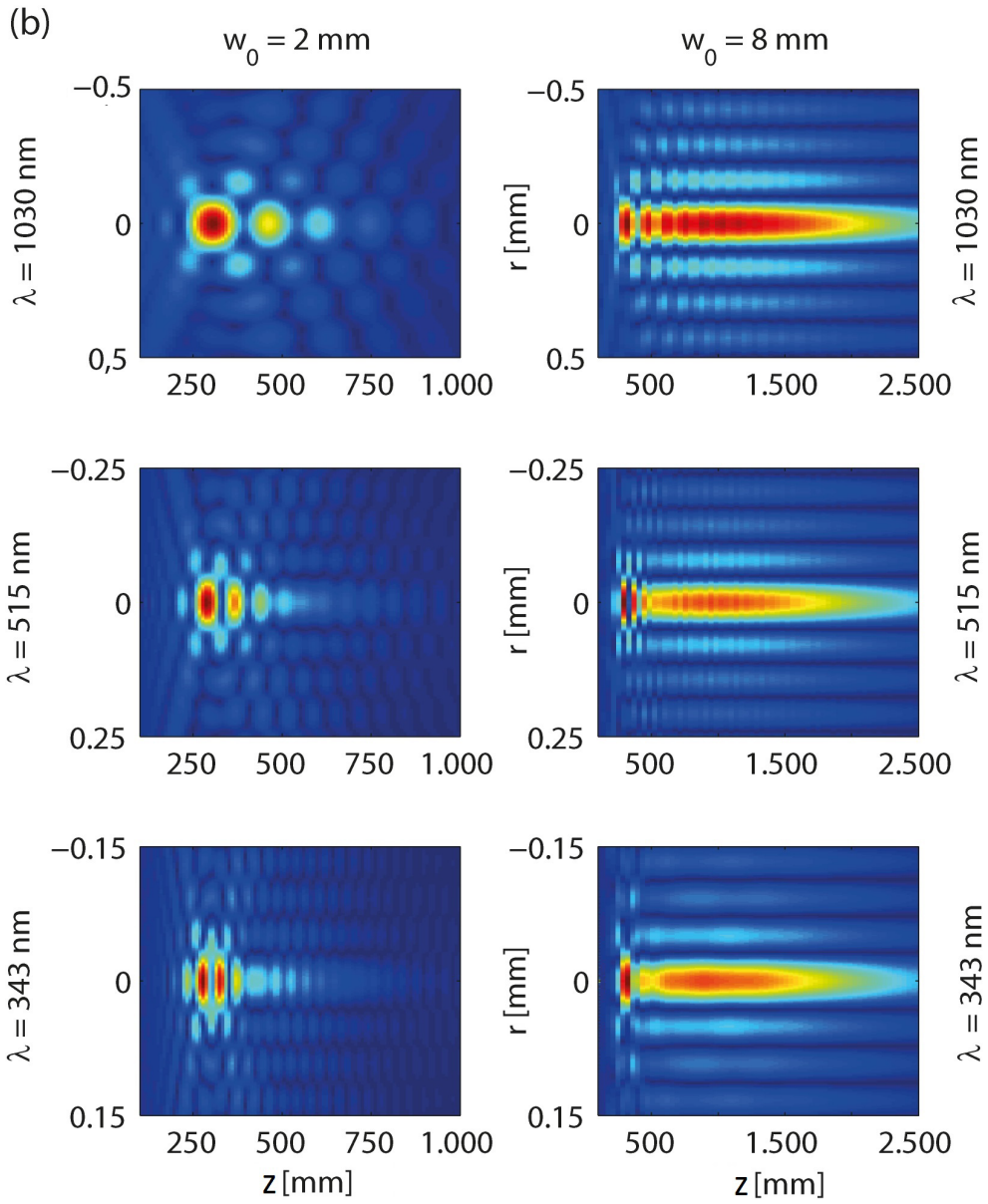

Figure 4. Continued.

center. Therefore, their intensities are $I(r=0,z)=0$, and they are composed of concentric rings in which the innermost ring has the maximum intensity. The electric field profile of Bessel vortex beams in the transverse plane is given by the Bessel function of first kind (J_n). The diameter of the innermost ring increases with indices of n. Since these beams do not show spectacular differences, excluding the diameter of the innermost ring, only J_1 was taken into account for this analysis. Based on these calculations, when the diameter of the innermost ring increases, they are less affected by axicon bluntness. Figure 6 shows the calculated intensity profile of a Bessel vortex beam in the transverse plane and its propagation characteristics for an ideal axicon. For example, a very long light pipe can be obtained for optical tweezers and particle-guiding applications. In addition, by adjusting the incoming beam energy, one can control the number of rings for interaction with sample in material-processing applications [25]. In order to explore the effect of axicon bluntness, the input

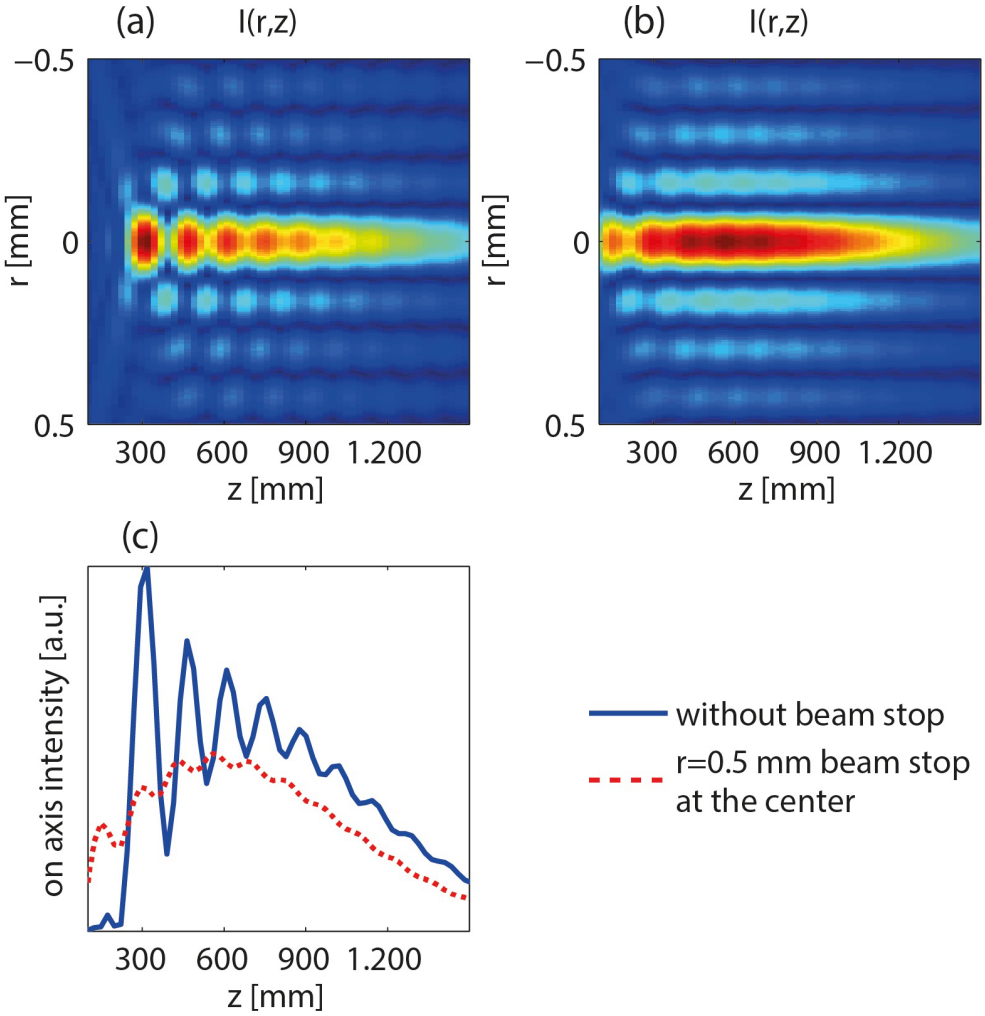

Figure 5. Intensity distributions for blunt-tip axicon a) without and b) with beam stop at the center where $\lambda = 1030$ nm and $w_0 = 5$ mm. c) $I(r = 0, z)$ values of a) and b) where the radius (r) of the beam stop is 0.5 mm.

beam waist was decreased and the Fresnel–Kirchhoff integral was investigated for a blunt axicon. As seen in Figure 7, a round axicon tip behaves like a commercial lens, focusing the input beam around 290 mm in the longitudinal position, which is very convenient considering the results in the previous section. Zero was also obtained on axis intensity behind the axicon in this calculation.

When the input beam size is very close to radius of the axicon tip, the effect of tip bluntness would appear in the intensity profile. In contrast, if the input beam waist is much higher than the axicon tip radius, intensity modulations are naturally much reduced. Another advantage of using a Laguerre–Gaussian beam for an input is that they also have a singularity at the center, and this property reduces intensity oscillations in the propagation direction. In order to prove this, the Fresnel–Kirchhoff integral was evaluated for a variety of input beam radii.

In this calculation, the axicon is again modeled as mentioned above. The results were compared with an ideal axicon. Figure 8 shows intensities in both the transverse and the longitudinal directions. As expected, when the beam waist increases, the overall beam profile approaches an ideal case. Calculations were extended to lower wavelengths (515 and 343 nm) to span a variety of applications.

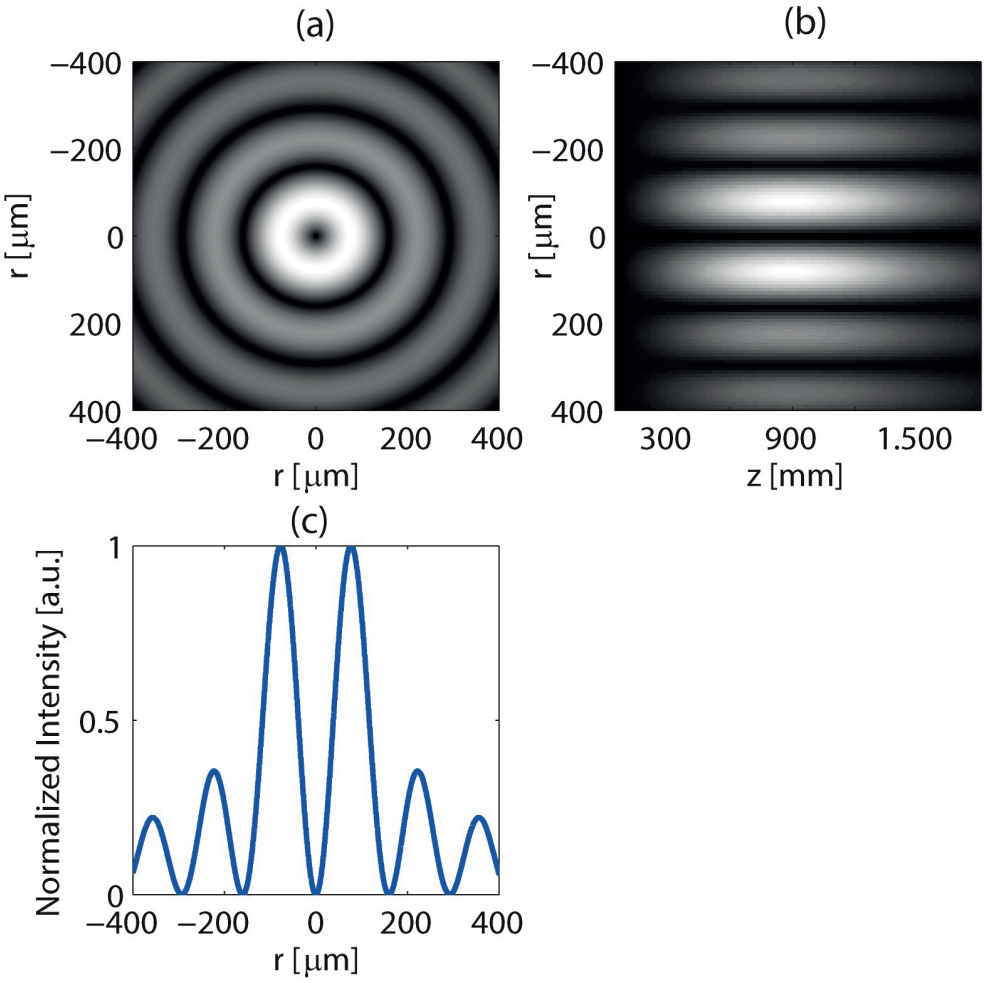

Figure 6. a) Bessel vortex beam profile in the transverse plane. b) Intensity distribution in the propagation direction and c) its cross-section at focal point of Bessel vortex beam, where $w_0 = 4$ mm, $\lambda = 1030$ nm axicon is modeled as an ideal.

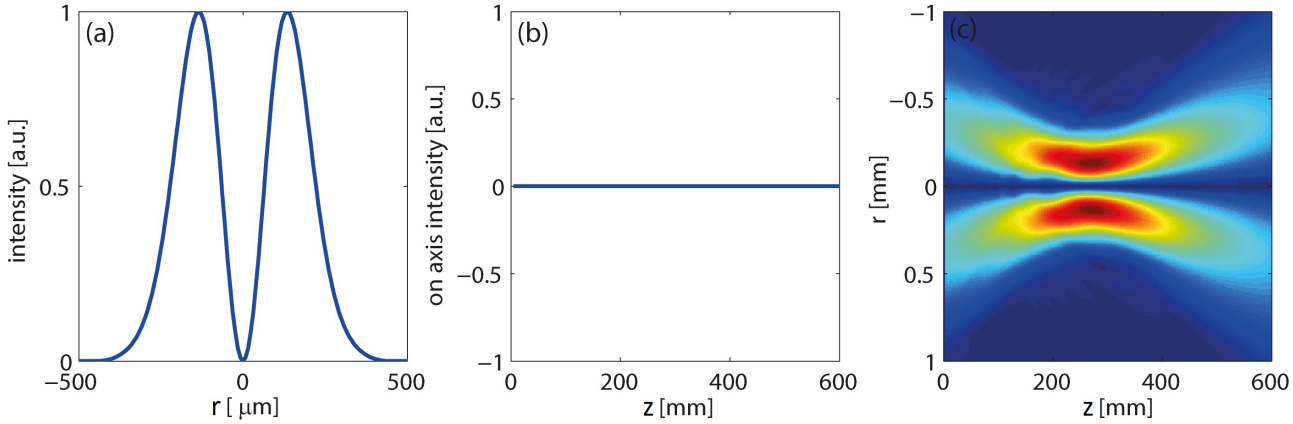

Figure 7. a) $I(r)$ at $z = 289$ mm, b) on axis intensity, and c) $I(r, z)$ values for $w_0 = 0.5$ mm, $\lambda = 1030$ nm, and a round-tip axicon.

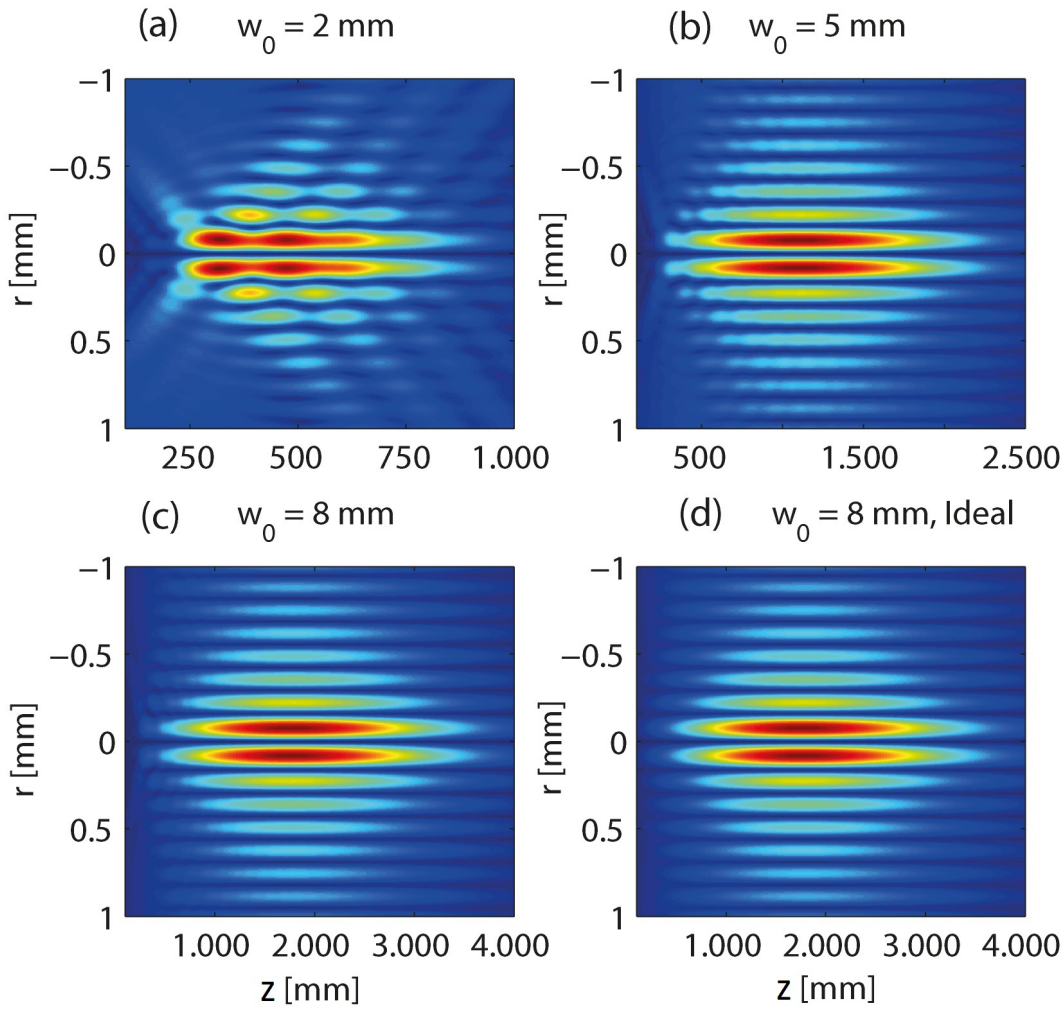

Figure 8. a), b), c) Intensities of Bessel vortex beams generated by blunt-tip axicons and d) ideal axicon for different input beam sizes (w_0), where $\lambda = 1030$ nm.

In this part, the beam waist was kept at 4 mm while the wavelength of the incoming light was changed. The obtained results are presented in Figure 9. The intensity profile of the Bessel beam approaches an ideal case as the wavelength of the laser beam gets smaller. Deviations from an ideal Bessel and Bessel vortex beams stem from the bluntness of the axicon tip, although Bessel vortex beams are less sensitive. However, a small variation is obtained for Bessel vortex beams and stopping the beam at the center can be applied in this case in order to remove intensity oscillations behind the axicon. In addition, energy loss is much reduced spontaneously in this case due to the singularity at the beam center.

Figure 10 shows the electrical field profiles of Bessel vortex beams obtained by using different input beam parameters. In this calculation, the wavelength of illuminating beam is taken as 1030 nm and the base angle of the axicon is 0.5° for the blunt case. The results clearly indicate that as the beam waist increases oscillations in the intensity profile decrease. Similarly, when the beam stop at the center is applied (left column to right column) before the axicon, the calculated beam profiles resemble the beam profiles obtained by using the same parameters for an ideal axicon.

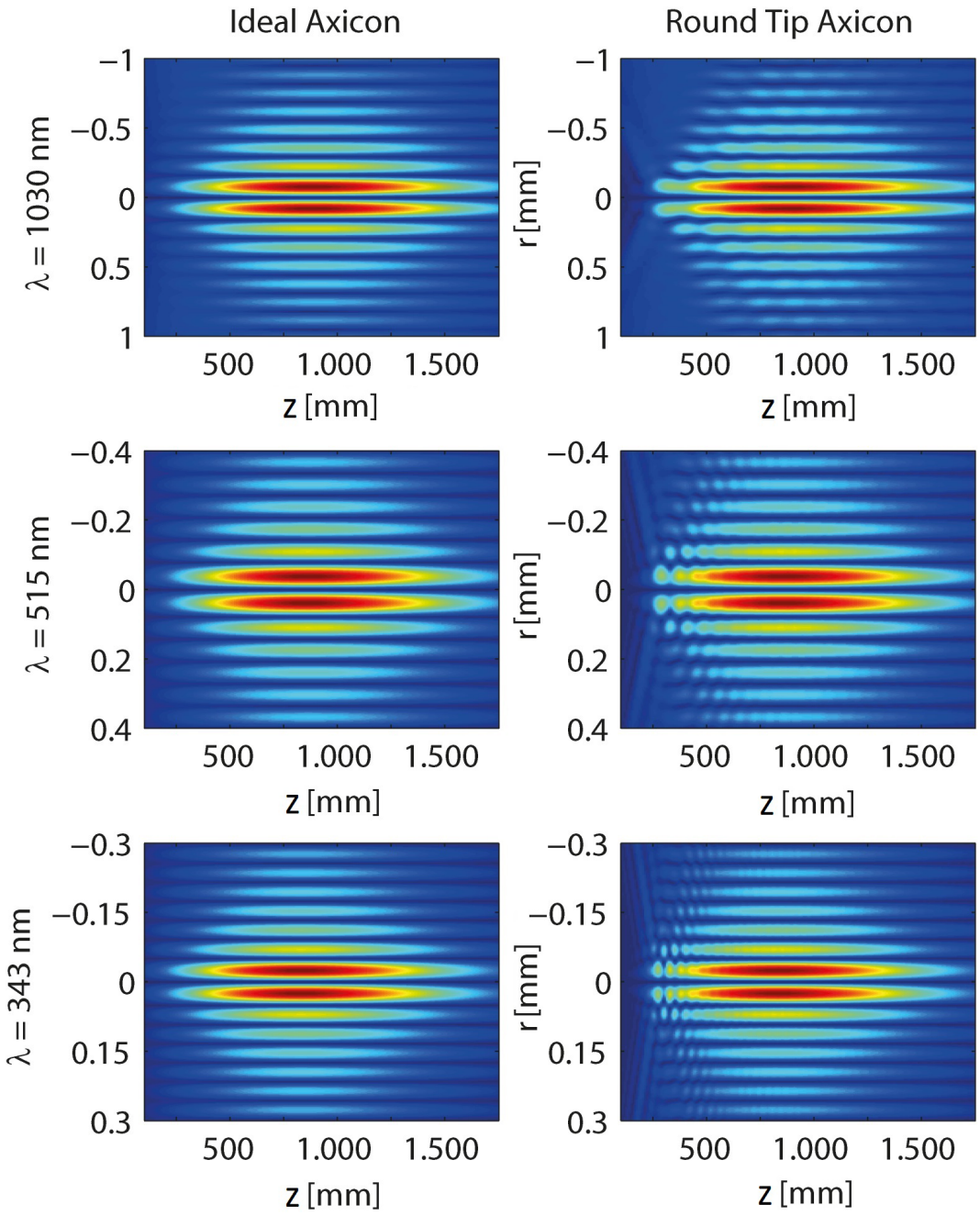

Figure 9. Intensity distributions of Bessel vortex beams generated by ideal axicon (left column) and blunt-tip axicon (right column) for different wavelengths where $w_0 = 4$ mm.

In order to compare the intensity cross-section of Bessel vortex beams generated by a blunt-tip axicon, intensity cross-sections were first evaluated for an ideal and a blunt-tip axicon without/with beam stop at the center. Then the beam waist of the incoming beam light was increased, while keeping all the other parameters constant. The results are summarized in Figure 11. Either increasing the input beam radius or stopping a small part of the input beam at the center enhances the quality of beam shaping.

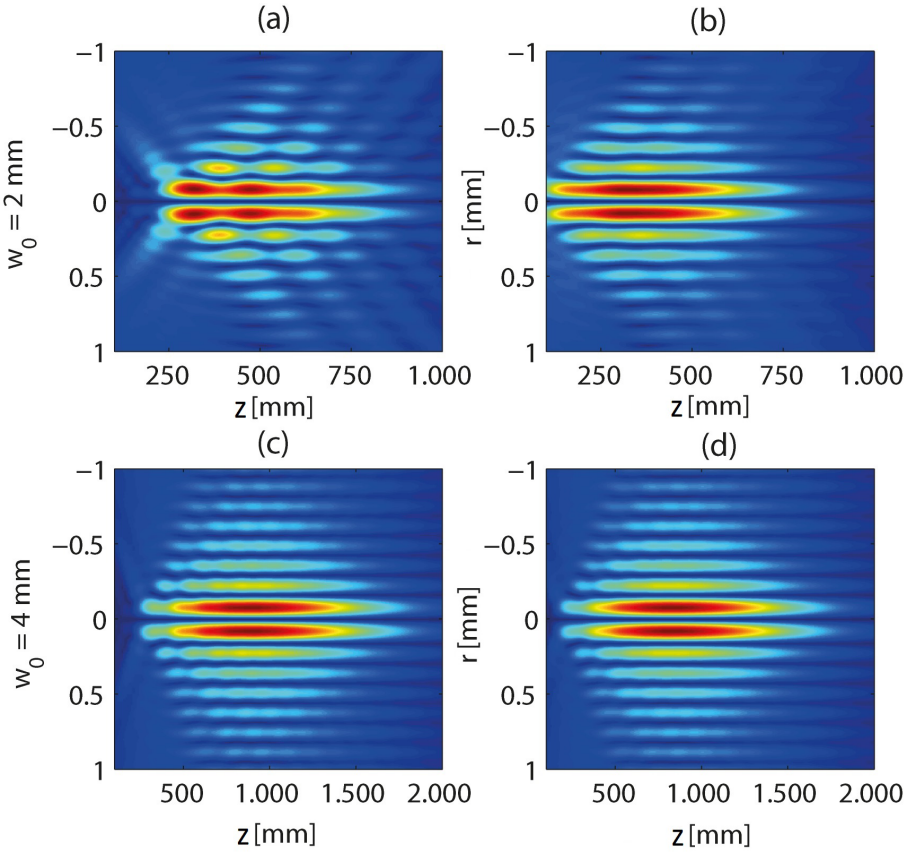

Figure 10. Intensity distributions of Bessel vortex beams for $w_0 = 2$ mm a) without beam stop and b) with beam stop, and for $w_0 = 4$ mm c) without beam stop and d) with beam stop. The radius of beam stop is 0.5 mm where the axicon tip is modeled as round.

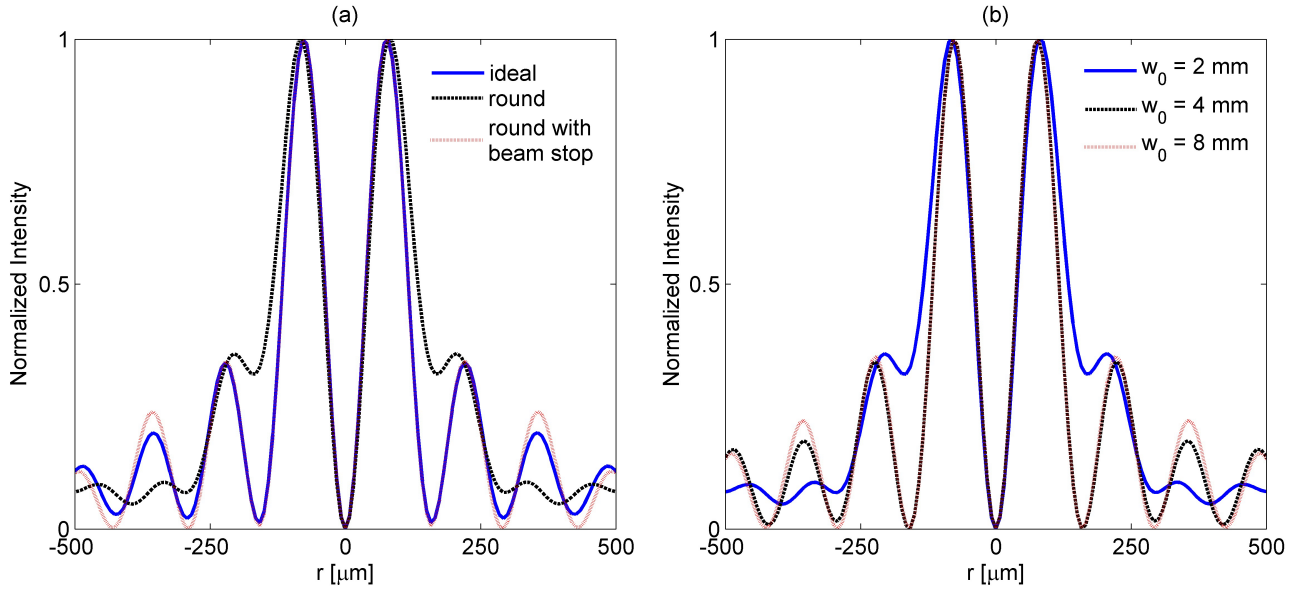

Figure 11. a) Intensity distributions of Bessel vortex beams for $w_0 = 2$ mm, $\lambda = 1030$ nm, and $\alpha = 0.5^\circ$. The radius of beam stop is 0.5 mm. b) Calculated intensities of Bessel vortex beams for a round-tip axicon. In this calculation, $\lambda = 1030$ nm, $\alpha = 0.5^\circ$, and different w_0 values are used.

3. Conclusions

The effects of axicon tip bluntness on generating Bessel and Bessel vortex beams were investigated for different input beam parameters. Systematic calculations clearly show that one can reduce intensity oscillations due to axicon roundness by optimizing input beam parameters or by stopping the input beam with a small portion at the center, paving the way for a small energy loss. Since they have a singularity at the center, Bessel vortex beams are less prone to intensity oscillations in the propagation direction. These results presented here emphasize the importance of optimizing input beam parameters in order to enhance quality of beam shaping by minimizing intensity oscillations in the propagation direction for a variety of applications.

Acknowledgments

This work was supported by the Scientific Research Projects Coordination Unit of Akdeniz University. Project Number: FAY-2017-2530. The authors thank Dr Timur Şahin for useful discussions.

References

[1] Durnin, J.; Miceli, J. J.; Eberly, J. H. *Phys. Rev. Lett.* **1987**, *58*, 1499-1501.

[2] Duocastella, M.; Arnold, C. B. *Laser Photon. Rev.* **2012**, *6*, 607-621.

[3] Arlt, J.; Dholakia, K. *Opt. Commun.* **2000**, *177*, 297-301.

[4] McGloin, D.; Dholakia, K. *Contemp. Phys.* **2005**, *46*, 15-28.

[5] Lee, K. S.; Rolland, J. P. *Opt. Lett.* **2008**, *33*, 1696-1698.

[6] Curatolo, A.; Munro, P. R. T.; Lorenser, D.; Sreekumar, P.; Singe, C. C.; Kennedy, B. F.; Sampson, D. D. *Sci. Rep.* **2016**, *6*.

[7] Garces-Chavez, V.; McGloin, D.; Melville, H.; Sibbett, W.; Dholakia, K. *Nature* **2002**, *419*, 145-147.

[8] Cizmar, T.; Kollarova, E.; Bouchal, Z.; Zemanek, P. *New J. Phys.* **2006**, *8*.

[9] Rioux, M.; Tremblay, R.; Belanger, P. A. *Appl. Opt.* **1978**, *17*, 1532-1536.

[10] Courvoisier, F.; Zhang, J.; Bhuyan, M. K.; Jacquot, M.; Dudley, J. M. *Appl. Phys. A.* **2013**, *112*, 29-34.

[11] Durfee, C. G.; Milchberg, H. M. *Phys. Rev. Lett.* **1993**, *71*, 2409-2412.

[12] Akturk, S.; Zhou, B.; Franco, M.; Couairon, A.; Mysyrowicz, A. *Opt. Commun.* **2009**, *282*, 129-134.

[13] Johannisson, P.; Anderson, D.; Lisak, M.; Marklund, M. *Opt. Commun.* **2003**, *222*, 107-115.

[14] Pyragaite, V.; Regelskis, K.; Smilgevicius, V.; Stabinis, A. *Opt. Commun.* **2006**, *257*, 139-145.

[15] Arnold, C. L.; Akturk, S.; Mysyrowicz, A.; Jukna, V.; Couairon, A.; Itina, T.; Stoian, R.; Xie, C.; Dudley, J. M.; Courvoisier, F. et al. *J. Phys. B At. Mol. Opt. Phys.* **2015**, *48*.

[16] Sahin, R.; Morova, Y.; Simsek, E.; Akturk, S. *Appl. Phys. Lett.* **2013**, 102.

[17] Sahin, R.; Kabacelik, I. *Appl. Phys. A* **2016**, *122*, 1-6.

[18] Sahin, R.; Simsek, E.; Akturk, S. *Appl. Phys. Lett.* **2014**, *104*.

[19] Sahin, R.; Akturk, S.; Simsek, E. *Appl. Phys. A* **2014**, *116*, 555-560.

[20] Gil-Villalba, A.; Xie, C.; Salut, R.; Furfaro, L.; Giust, R.; Jacquot, M.; Lacourt, P. A.; Dudley, J. M.; Courvoisier, F. *Appl. Phys. Lett.* **2015**, *107*.

[21] Vasara, A.; Turunen, J.; Friberg, A. T. *J. Opt. Soc. Am. A. Opt. Image Sci. Vis.* **1989**, *6*, 1748-1754.

[22] Indebetouw, G. *J. Opt. Soc. Am. A. Opt. Image Sci. Vis.* **1989**, *6*, 150-152.

[23] Courvoisier, F.; Lacourt, P. A.; Jacquot, M.; Bhuyan, M. K.; Furfaro, L.; Dudley, J. M. *Opt. Lett.* **2009**, *34*, 3163-3165.

[24] McLeod, J. H. *J. Opt. Soc. Am.* **1954**, *44*, 592-597.

[25] Sahin, R.; Ersoy, T.; Akturk, S. *Appl. Phys. A.* **2014**, *118*, 125-129.

[26] Wetzel, B.; Xie, C.; Lacourt, P. A.; Dudley, J. M.; Courvoisier, F. *Appl. Phys. Lett.* **2013**, *103*.

[27] Brzobohatý, O.; Cizmár, T.; Zemánek, P. *Opt. Express.* **2008**, *16*, 12688-12700.

[28] Akturk, S.; Zhou, B.; Pasquiou, B.; Franco, M.; Mysyrowicz, A. *Opt. Commun.* **2008**, *281*, 4240-4244.

[29] Wu, P.; Sui, C.; Huang, W. *Photon. Res.* **2014**, *2*, 82-86.

[30] Dépret, B.; Verkerk, P.; Hennequin, D. *Opt. Commun.* **2002**, *211*, 31-38.